J. Min. Metall. Sect. B-Metall. 53 (3) B (2017) 271 - 278

Journal of Mining and Metallurgy, Section B: Metallurgy

PHASE FIELD CRYSTAL SIMULATION OF THE STRUCTURE EVOLUTION BETWEEN THE HEXAGONAL AND SQUARE PHASES AT ELEVATED PRESSURES

X. Shuai, H. Mao, Y. Kong *, Y. Du **

State Key Lab of Powder Metallurgy, Central South University, Changsha, Hunan, China

(Received 27 May 2017; accepted 11 September 2017)

Abstract

Based on the two-mode phase field crystal (PFC) model and the principle of the common tangent, a two-dimensional PFC phase diagram is established. According to the phase diagram, the parameters for a steady growth of the hexagonal and the square phase are found. Moreover, the nucleation and growth characteristics of the square phase from hexagonal phase under different pressures are simulated by using these parameters. The movements of dislocation core under pressure at different transformation stages are revealed and compared with each other. Finally, by changing the grain orientation, the formation and disappearance of grain boundaries at different angles are simulated and analyzed.

Keywords: *Two-mode phase field crystal model; Nucleation and growth characteristics; Pressure; Grain orientation.*

1. Introduction

Materials under different heat treatments will lead to different microstructure, and the microstructure, such as the size, distribution and orientation of grain, as well as interfacial structure etc., determines the comprehensive mechanical properties of the material. As an independent physical parameter besides temperature, pressure can induce structural transition and lead to the formation of new high pressure structure, which provides an effective method to explore new structure, new property and new phenomenon. However, in contrast to temperature induced transition, except for a few low pressure researches, the experimental investigation employing high pressure is limited. For example, the higher pressure research in VO_2 (M1) [1] and the research on other initiating structure is unavailable [2]. Therefore, the detail of high-pressure structural phase transitions in micro and nano size scale is still not very clear. Just like that although it is known that the phase transition process usually includes nucleation and growth, it is a challenge to directly observe atomic migration trajectory under high pressure experimentally.

With the rapid development of computer technology, numerical simulation has become an important tool in materials science. Among the available models, the traditional phase-field method has recently emerged as a powerful numerical method for studying the evolution of microstructure. For example, Yang *et al.* predicted the kinetic phase diagrams in the Si-As system by using the phase-field simulation with the time-elimination relaxation scheme [3]. Uehara [4] proposed a phase field model for predicting deformation behavior under an applied stress. Furthermore, through phase field simulation, Mamivand *et al.* [5] showed that external stress favors the formation of monoclinic variants, which exhibit transformation strains aligned with the applied stress direction. These successfully applied phase-field methods, however, neglect the periodic arrangement of atoms [6-9]. Consequently, it is difficult to reflect the structural characteristics of the crystal structure and atomic scale behavior of materials by means of the traditional phase field method.

Recently, the phase field crystal (PFC) method established by Elder et al. has emerged as an attractive computational approach to simulate the evolution of crystalline patterns [8-15]. Crystal morphology varies observably with the ordering condition, encompassing the faceted structures to symmetric dendrites, which in turn produces an equally diverse range of physical properties [10, 11]. The PFC model proposed by Elder et al. is based on classical density functional theory, which introduces a sequence-local atomic density

Dedicated to the memory of Professor Dragana Živković

*Corresponding author:*yikong@csu.edu.cn,**yong-du@csu.edu.cn*

DOI:10.2298/JMMB170527027S

field function containing periodic characteristics. The atomic density field of the liquid phase is a constant value, while the density field of the solid phase is expressed as a periodic function (wave) and the lattice structure of the crystal is expressed by the atomic density function of the period. It is natural to closely relate to the physical properties produced by the periodic structure to the related microstructure feature, such as the elastic effect, the grain orientation and the movement of the dislocations [12-15]. Following Elder et al.'s work, Greenwood et al.[10] introduced a new particle association function based on the density functional theory and constructed a PFC model for the transformation of the square phase structure. On the other hand, Wu et al. [16] proposed a two-mode PFC model which can describe a more complex crystal lattice structure than previous PFC model, including square lattice, face-centered cube (FCC) lattice *etc.*. The two-mode PFC provides a new strategy for the study of complex lattice transformation.

The PFC model, which is based on classic density functional theory, can be used to simulate the dynamics of microstructural evolution from atomic scale, just like molecular dynamics (MD) simulations. Moreover, one of the advantage of PFC over MD is that PFC model usually applied in the scale of diffusion time [16]. At present, however, the effect of pressure on microstructure transition has not been systematically studied by two-mode PFC method. Since choosing a suitable pressure is important for regulating microstructure, it is meaningful to study the effect of pressure on grain nucleation and growth at atomic scale and diffusion time scale with two-mode PFC method.

In this work, the effect of applying different pressure on the transformation from hexagonal phase into the square phase is studied systematically. In addition, the influence of pressure on the early stage of hexagonal phase formation, growth period of square phase and the corresponding structural transformation are analyzed. The outline of this paper is as follows. Firstly, the two-mode PFC model is described in Section 2. Then, the effect of pressure on the precipitation and growth of the square phase was discussed in Section 3. Besides, the effect of pressure on grain boundaries at different angles was studied. Finally, the conclusions resulting from the present work are presented in Section 4.

2. The phase field crystal model and simulation description

2.1 The free energy function

Like classical density-function theory (DFT), the PFC method is based on representing the free energy of a material by a functional of its density field. In this work, a "two-mode" phase-field-crystal model is used, which starts the free energy functional as:

$$F=\int\left[\frac{n}{2}\left\{\begin{matrix}-r+(\nabla^2+1)^2\times\\ \left[R_1+(\nabla^2+Q_1^2)^2\right]\end{matrix}\right\}n+\frac{n^4}{4}\right]dV=\int F_0 dV \quad (1)$$

where n and r represent dimensionless atomic number density and temperature parameter, respectively. In addition, the relative amplitudes of those density waves can be varied by varying R_1. Q_1 is a coefficient which represents the ratio of second Brillouin district and first Brillouin one. With the decrease of R value, the model will approach to the two-mode approximation gradually. In order to simulate the square phase, two characteristic parameters (R_1=0, $Q_1=\sqrt{2}$) are fixed. Thus the free energy density function F_0 for square phase can be written as follows

$$F_0=\frac{4-r}{2}n^2+\frac{n}{2}\left(\begin{matrix}\nabla^8+6\nabla^6+\\ 13\nabla^4+12\nabla^2\end{matrix}\right)n+\frac{n^4}{4} \quad (2)$$

2.2 Kinetic equation

As a conserved order parameter, the temporal evolution of the atomic number density field n obeys the following Cahn-Hilliard equation [17]:

$$\frac{\partial \mathrm{n}}{\partial t}=\nabla^2\frac{\delta F_0}{\delta n}+\xi \quad (3)$$

where ξ represents Gaussian random noise and the effect of this term on the first degree of n is ignored in this work. The PFC dynamic equation is established by inserting Eq. (2) into Eq. (3):

$$\frac{\partial n}{\partial t}=\left[\begin{matrix}\nabla^{10}+6\nabla^8+13\nabla^6+\\ +12\nabla^4+(4-\varepsilon)\nabla^2\end{matrix}\right]n+\nabla^2 n^3 \quad (4)$$

The Fourier method is used to deal with the boundary conditions. The Laplace operator can be effectively processed by Fourier spectra. In this study, semi-implicit pseudo-spectral method was selected. The discrete form of kinetic equation shown in Eq. (3) is as follows:

$$\frac{\tilde{n}_{\vec{k},t+\Delta t}-n_k}{\Delta t}=\left[\begin{matrix}-k^{10}+k^8-13k^6+\\ 12k^4-(4-r)k^2\end{matrix}\right]\tilde{n}_{k,t+\Delta t}-k^2\tilde{n}_k^3 \quad (5)$$

In order to facilitate the calculation, we further organize the above formula as:

$$\tilde{n}_{k,t+\Delta t}=\frac{(n_k-k^2\Delta t\tilde{n}_k^3)}{1-\Delta t\left[\begin{matrix}-k^{10}+k^8-13k^6+\\ +12k^4-(4-r)k^2\end{matrix}\right]} \quad (6)$$

where $\tilde{n}$ is the expression obtained by the Fourier transform of the atomic density field n, and k is the Fourier space wave vector.

2.3 Calculation detail

To examine the equilibrium properties of this two-

mode PFC model, we construct the phase diagram, which is obtained by computing the free-energy density as a function of the mean density n_0 in solid and liquid. The free energy curves of the square phase are calculated using the two-mode approximation of the density fields:

$$n = \sum A_{i,j} e^{2\pi \vec{G}_{i,j} \cdot \vec{r}} + n_0 \tag{7}$$

where G is the reciprocal vector, r is the spatial position vector, and $A_{i,j}$ is the Fourier coefficient. The first term in Eq. (7) reflects the structural characteristics associated with the periodic arrangement of the lattice atoms, and the second term is a constant reflecting the mean atomic density of the disordered phase.

The two-dimensional PFC model can be used to represent different phases such as liquid, stripe, hexagonal and square. In order to establish two-dimensional PFC phase diagram, the free energy of each phase was calculated. The appropriate expression of the atomic density function is found, which inserts into its free energy to find the suitable form. The two-dimensional PFC phase diagram is then obtained according to the comment tangent of the free energies.

In the case of a single mode PFC model, the liquid phase, stripe and hexagonal phases are represented as follows [18, 19].

The liquid phase:

$$n = n_l = n_0 \tag{8}$$

The stripe phase:

$$\begin{aligned} n &\approx n_l + \sum A_{i,j} e^{i\vec{G}_{i,j} \cdot \vec{r}} \\ &= 2A_l \cos q_l x + n_0 \end{aligned} \tag{9}$$

The hexagonal phase:

$$\begin{aligned} n &\approx n_h + \sum A_{i,j} e^{i\vec{G}_{i,j} \cdot \vec{r}} \\ &= 2A_h \left[\cos(q_h x) \cos \cdot \frac{q_h}{\sqrt{3}} y + \frac{1}{2} \cos(\frac{2q_h}{\sqrt{3}} y) \right] + n_0 \end{aligned} \tag{10}$$

For the two-mode PFC model, the square phase is described by an equation of the form[20]:

$$\begin{aligned} n &\approx n_s + \sum A_{i,j} e^{i\vec{G}_{i,j} \cdot \vec{r}} \\ &= n_0 + 2A_s (\cos q_s x + \cos q_s y) + \\ &\quad + 4B_s \cos q_s x \cos q_s y \end{aligned} \tag{11}$$

These density functions will be brought into their respective free energy functions for the integral operation, during which the expression of the free energy function will be solved as:

The liquid phase:

$$f_l = (4 - r) \frac{n_0^2}{2} + \frac{n_0^4}{4} \tag{12}$$

The stripe phase:

$$f_{st} = -\frac{5}{4} n_0^4 + \frac{4 + r}{2} n_0^2 - \frac{r^2}{6} \tag{13}$$

The hexagonal phase:

$$\begin{aligned} f_h = &\frac{n_0}{4} + \frac{4 - r}{2} n_0^2 + \frac{45}{2} A_h^4 - \\ &- 12 n_0 A_h^3 + (9 n_0^2 - 3r) A_h^2 \end{aligned} \tag{14}$$

where

$$A_h = \frac{4}{5} (n_0 + \frac{1}{3} \sqrt{-15r - 36 n_0^2}); q_h = \frac{\sqrt{3}}{2}$$

The square phase:

$$\begin{aligned} f_s = &\frac{4 - r}{2} n_0^2 + \frac{1}{4} n_0^4 + (-2r + 6 n_0^2) A_s^2 \\ &+ (-2r + 6 n_0^4) B_s^2 + 9 A_s^4 + 9 B_s^4 \\ &+ 36 A_s^2 B_s^2 + 24 n_0 A_s^2 B_s \end{aligned} \tag{15}$$

where

$$A_s = \frac{1}{9P} \begin{bmatrix} r^2 + 75 n_0^4 - 2 n_0 Q + 4 r n_0^2 + \\ + (5r - 31 n_0^2) P^2 + P^4 - 10 n_0^3 P - \\ - 2 r n_0 P + \sqrt{3} (r^2 + 75 n_0^4 - 2 n_0 Q + \\ + 4 r n_0^2 - P^4 + 10 n_0^3 P + 2 r n_0 P) i \end{bmatrix}^{1/2}$$

$$B_s = -\frac{1}{18P} \begin{bmatrix} r + 5 n_0^2 + 8 n_0 P + P^2 + \\ + \sqrt{3} (P^2 - 5 n_0^2 - r) i \end{bmatrix}$$

and

$$P = \left(3 r n_0 + \left(\sqrt{\begin{matrix} -r^2 - 6 r^2 n_0^2 - \\ -225 r n_0^4 + 500 n_0^6 \end{matrix}} \right) - 25 n_0^3 \right)^{1/3}$$

$$Q = \sqrt{-r^3 - 6 r^2 n_0^2 - 225 r n_0^4 + 500 n_0^6}$$

2.4 Construction of a phase diagram

The equilibrium of the two phases should meet the conditions of chemical equilibrium, thermal equilibrium, and mechanical equilibrium. Thus, it requires that in the two-phase region, the chemical potential, temperature and pressure are equal. Under such conditions, the two-phase coexistence region can be found. Specifically, pressure can be considered as a unit of volume of the giant thermal potential. If the giant thermal potential is equal, pressure will be identical. Besides, it should meet the conditions that temperature is equal at (n_0, r) point. Therefore, the chemical potential and the giant thermal potential should be equal too. Based on the principle of common tangent, the two-dimensional PFC phase diagram is calculated and plotted by using Eqs. 12-15, and the results are shown in Fig. 1.

3. Results and discussion

3.1 Structure transformation at zero pressure

Materials may show different microstructures under different environments. In this work, a set of

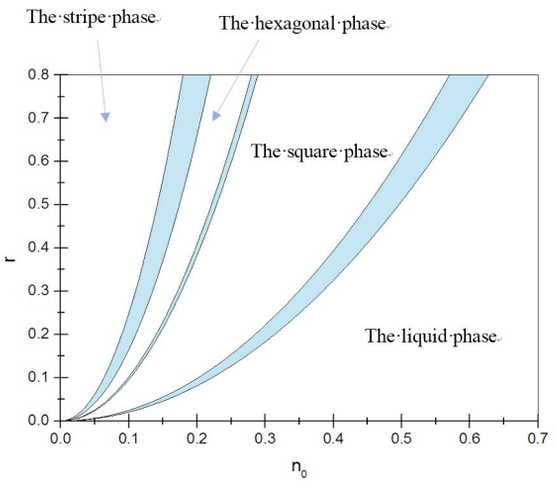

Figure 1. *Phase diagram of the two-mode PFC model for R_1=0 computed using two-mode and one-mode expansions of the crystal density field for square and hexagonal phase, respectively. The light blue part represents the two-phase coexistence zone.*

samples under normal pressure were prepared with PFC simulations. The point (n_0,r) = (0.21, 0.15) in the established two-mode PFC phase diagram is selected. As show in Fig. 1, this point is in the region where the square phase grows steadily and the liquid and hexagonal phases are metastable. In order to speed up the nucleation of the process, a few random nuclei were selected. The corresponding parameters are listed in Table 1. Except for the nuclei, the other areas are set to be liquid phase, as shown in Fig. 2a.

Table 1. *Dimensionless sample initialization parameter.*

No.	1	2	3	4	5	6	7	8
radius	8	10	14	16	20	21	30	35
angle	30	60	55	22.5	40	58	45	63

The nuclei and growth processes of the hexagonal phase are shown in Fig. 2. The hexagonal grains are nucleated in the liquid phase (Fig. 2a). As time evolves, the grains grow slowly until they come into contact with other hexagonal grains (Fig. 2b). At this time, if the angle of orientation of the hexagonal phase before contact is large, the grain boundary will be formed. If the orientation angle difference is small, the grain boundaries will then merge, resulting in the passive formation of some dislocations.

When the evolution time reaches 15000 time steps, the nuclei of square phase are generated at the grain boundary of hexagonal phase. At the intersection of the three grains, the nuclei of square phase appeared at the fastest speed. Moreover, the square phase is more stable under the condition of the set parameters, which will devour the hexagonal grains and grow slowly. At the 42000 time steps, the

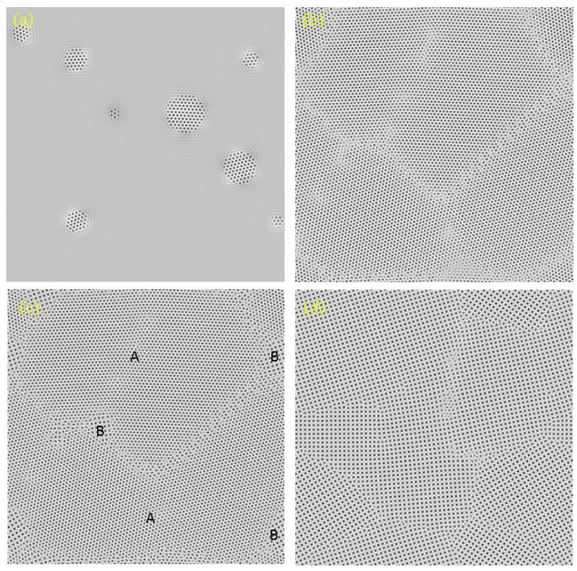

Figure 2. *Dynamical evolution of the original sample microstructure (a) sample at t=0; (b) sample at t=6000; (c) sample at t=15000; (d) sample at t=42000.A: hexagonal phase; B: square phase.*

entire area has been occupied by the square phase, meaning that the phase transformation process has completed. There are still dislocations in the grains boundary, which are shown in Fig. 2(d). Overall, it is observed that the new phases tend to be preferentially nucleated at the intersection of the three grains. While a small difference in grain orientation will lead to the formation of a small angle grain boundary. In addition, the hexagonal to square structure evolution simulated by PFC model is similar to that results from the molecular dynamics method. The free energy minimization curve during the transition process is shown in Fig. 3. The abscissa indicates the evolution time, and the fir coordinates represent the energy density. Each ladder represents a relatively stable state, the turning point represents the formation of the new phase or the disappearance of the previous phase.

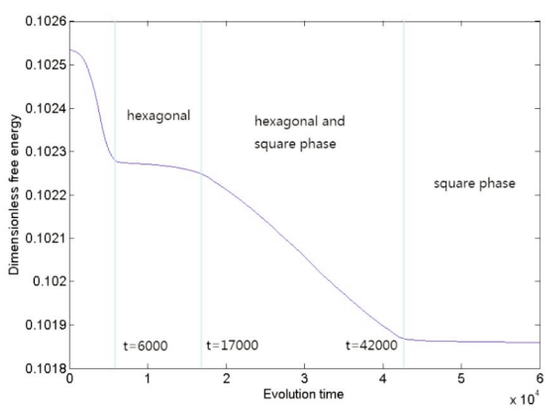

Figure 3. *The energy curve of the sample.*

3.2 Structure transformation at elevated pressures

To reveal the impact of pressure on structural transformation, the samples at the beginning of the present PFC simulation are the same as those used at section 3.1. In order to prevent the overpressure of the model from breaking, the pressurization process will be controlled gradually within 4800 steps. Therefore, the largest deformation is 4.8% when the pressurization process is completed.

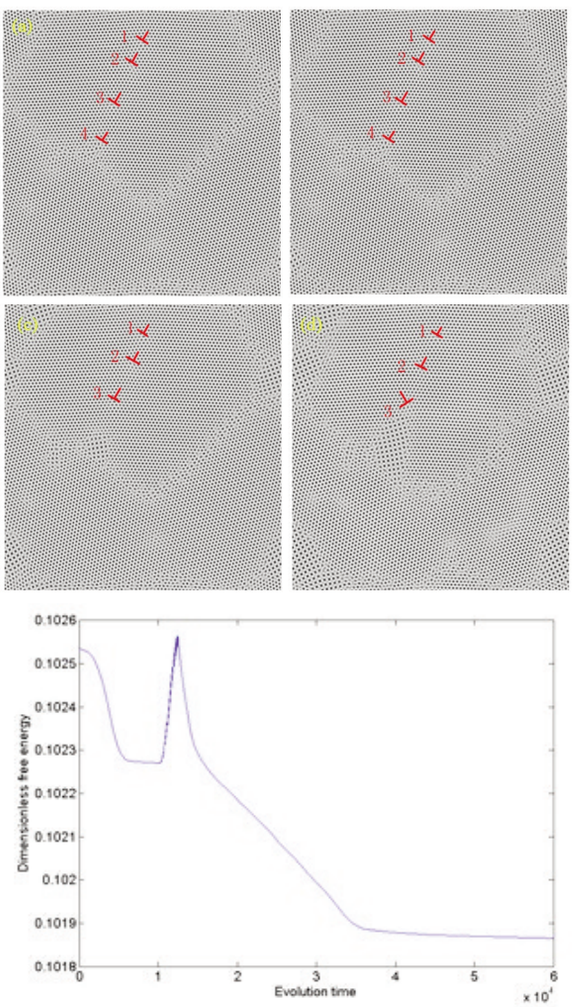

Figure 4. *Dynamic evolution of microstructures of the pressurized samples and the energy curve (a) sample at t=10000; (b) Pressurized sample at t=10000; (c) sample at t=15000; (d) Pressurized sample at t=15000; (e) The energy curve of the pressurized*

3.2.1 Pressurized at the early stage

To demonstrate the effect of pressurization on the quadratic nuclei visually, the first pressurization experiment is conducted before the quadratic nuclei and the hexagonal phase cover the region. The pressure was applied for 24 times and changed by 0.2% for each time. The results of the pressurization are shown in Fig. 4.

By comparing the simulation results under high pressure (Fig. 4 c and d) with zero pressure (Fig. 4 a and b), it can be found that the nucleation rate of the square phase can be enhanced remarkably by applying a certain amount of deformation during pressurization. Orientation also has a certain impact on the formation of the new square phase. When pressure is applied, the free energy of the sample increases (Fig. 4e). After a period of evolution, the free energy begins to decrease smoothly and then is evolved similar to that of the sample without pressurization.

3.2.2 Pressurized at the medium stage

After the nucleation, the effect of pressurization on the growth of square phase is studied. The applied pressure starts at 20000 steps, when a part of the square phase can be observed. The method for gradually applying pressure is consistent with the one used in section 3.2.1, and the results of the pressurization are shown in Fig. 5 b and d.

From the figure, one finds that the crystal morphology of the two sets of samples is consistent with each other before pressing (Fig. 5 a and b). After applying pressure, it can be seen that the positions of the grain boundary and the dislocation have changed significantly, as indicated in Fig. 5 c and d. In addition, by comparing the two sets of samples, it is observed that the growth rate of the square phase increased significantly in the sample under pressure. Fig. 5e shows the free energy curve of the two sets of experiments. When pressure is applied, the free energy of the sample increases significantly, and after a period of evolution, the free energy curve of the sample with pressurized is consistent with zero pressure samples.

3.2.3 Pressurized at the later stage

In order to observe the effect of pressure on the sample after phase transformation, pressure is applied to the sample when the structural transformation has been completed. With reference to the normal growth of the sample, where it is found that structural transition has been completed at 42000 time steps, pressure is applied after 45000 time steps at the later stage. The method for gradually applying pressure is consistent with the one used in section 3.2.1.

The samples before the pressurization are shown in Figs. 6 a and b, where the crystal morphology of the two sets of samples remained consistent. When the pressure was applied, the effect of the pressure on the sample that had completed the structural transformation was smaller than that in the previous

simulations. This is because the sample structure tends to maintain stable. Pressure mainly affects the action of the grain boundary and dislocation. The evolution results are shown in Figs. 6 c and d. The migration of the dislocation core is obvious, together with the creation of new dislocations, as shown in Fig. 6d. The position of the grain boundary also has some displacement along the direction of the pressure. The energy curve of the sample is shown in Fig. 6e, and the free energy of the sample after pressurization increases significantly and trends to be stable after a period of evolution.

3.2.4 The effect of grain orientation on structure transformation at elevated pressure

The effect of pressure on the sample after transformation has been studied in previous sections. However, the grain orientation of the structure after transformation is not controllable. Therefore, in this section, different initial grain orientations are set and then used for applying pressure.

In order to simplify the comparison, only two initial grains are selected, and the radius are set to be 12. The grain orientations of sample A are $\theta_1 = 0$, $\theta_2 = 5^o$, respectively, and the initial sample is shown in Fig. 7a. The grain orientations of sample B are $\theta_1 = 0$, $\theta_2 = 15^o$, respectively, and the initial sample is shown in Fig 7c. After a period of evolution, the two grains contact each other and form grain boundaries. The evolutionary results are shown in Figs. 7 b and d, respectively. The difference in orientation between the grains is small. So a small angle grain boundary is

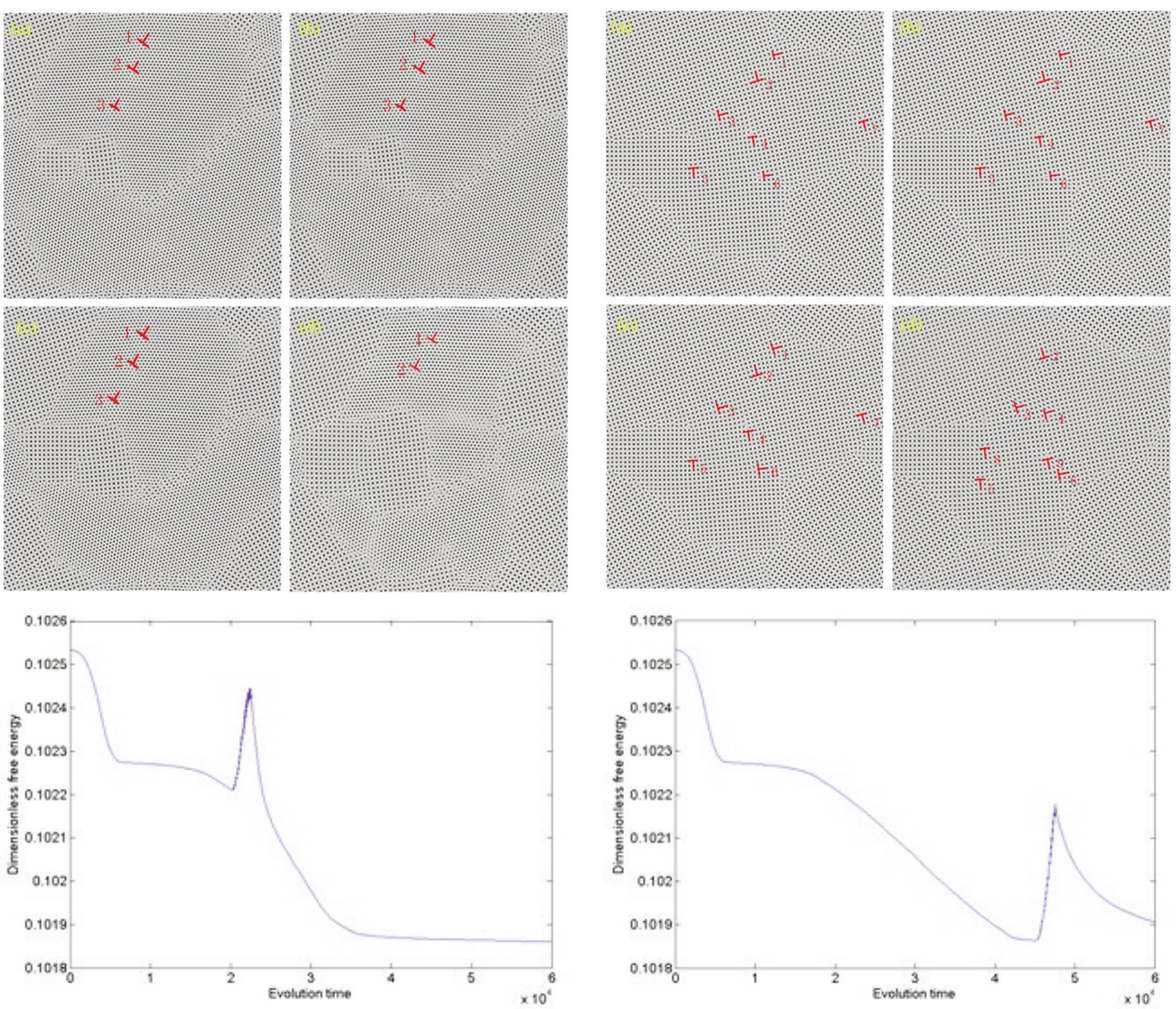

Figure 5. *Dynamic evolution of microstructures of the pressurized samples and the energy curve. (a) Control sample at t =20000; (b) Pressurized sample at t=20000; (c) Control sample at t=25000; (d) Pressurized sample at t=25000; (e) The energy curve of the pressurized sample.*

Figure 6. *Dynamic evolution of microstructures of the pressurized samples and the energy curve (a) Control sample: T=45000; (b) Pressurized sample: T=45000; (c) Control sample: T=50000; (d) Pressurized sample: T=50000; (e) The energy curve of the pressurized sample.*

formed (Fig. 7b). When the difference in orientation lowers to a certain extent, the grains are merged without forming a grain boundary. When the angle of orientation is greater than a certain value, a relatively stable large angle grain boundary is formed.

Two sets of samples are then subjected to pressurization simulations (Fig. 8). When the two grains begin to contact (Figs. 7 b and d), the pressure is applied to the sample. Changes in the two grain boundaries can be observed from the comparison between Fig. 8 b and d with Figs. 7 b and d. After the application of pressure, small orientation grain boundary between the two grains easily forms once the grain boundary rotation occurs, which will result in further reduction of the orientation difference and make the grain together, or expand the difference of orientation and become large angle grain boundaries. This is also the reason for the large grain boundary widespread in the sample.

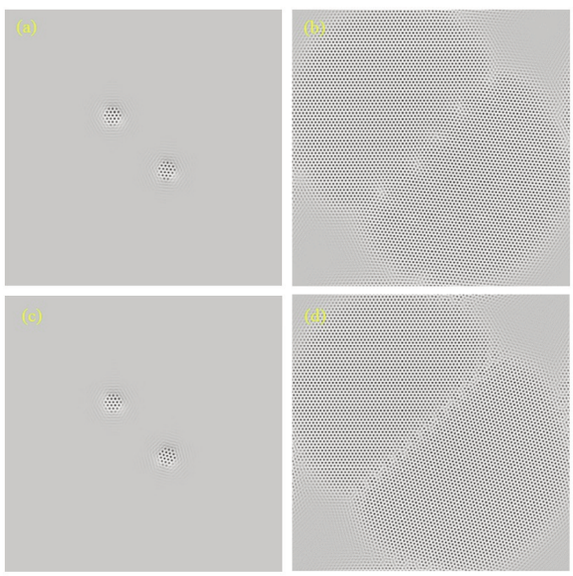

Figure 7. *The crystal morphology (a) Sample A: T=0; (b) Sample A: T=8000; (c) Sample B: T=0; (d) Sample B: T=8000.*

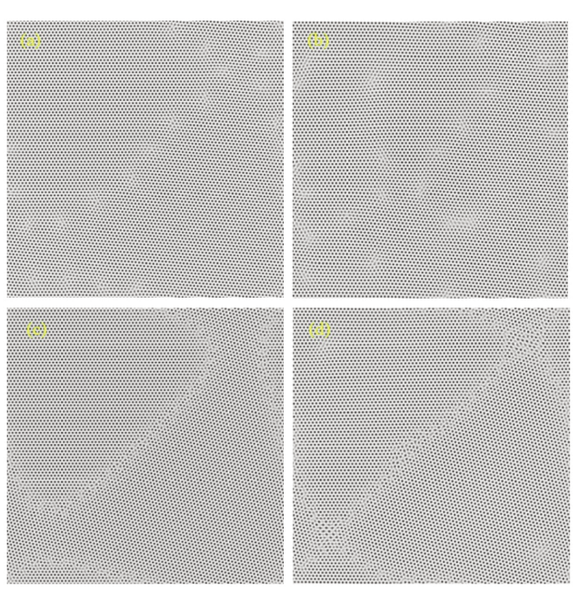

Figure 8. *The crystal morphology (a) Sample A: T=15000; (b) Pressurized sample A: T=15000; (c) Sample B: T=15000; (d) Pressurized sample B: T=15000.*

4. Conclusions

In conclusion, the two-mode PFC model is used to simulate hexagonal lattice transformation to square lattice structure at elevated pressures. And the influence of the grain orientation of the square phase after the structure transformation at elevated pressures is also discussed. The main conclusions are as follows:

(1) It is possible to increase the nucleation rate of the square phase and to influence the orientation of the generated square phase at elevate pressures.

(2) Pressure will cause the dislocation in grain and grain boundary migration.

(3) The appearing grain boundaries are related to the orientation of the initial nuclei and the applied pressure.

Acknowledgement

The financial support from National Natural Science Foundation of China (Grant No. 51531009) is greatly acknowledged.

References

[1] L.L. Fan, Y.F. Wu, C. Si, C.W. Zou, Z.M. Qi, L.B. Li, G.Q. Pan, Z.Y. Wu, Thin Solid Films, 520 (2012) 6124–6129.

[2] B. Cheng, Q. Li, H. Zhang, R. Liu, B. Liu, Z. Yao, T. Cui, J. Liu, Z. Liu, B. Sundqvist, Phys. Rev. B, 93 (2016).

[3] X. Yang, Y. Tang, D. Cai, L. Zhang, Y. Du, S. Zhou, J. Min. Metall. Sect. B-Metall. 52 (1) B (2016) 77-85

[4] T. Uehara, 124 Phase field modeling of phase transformation under an applied stress, The Proceedings of The Computational Mechanics Conference, 2008, pp. 404-405.

[5] M. Mamivand, M.A. Zaeem, H.E. Kadiri, Acta Mater., 64 (2014) 208-219.

[6] J. Wang, X. Wang, Q. Nie, Discrete. Cont. Dyn-B, 20 (2015) 3185-3213.

[7] A. Karma, W.J. Rappel, Phys. Rev. E, 53 (1996) R3017.

[8] G. Caginalp, P. Fife, Phys. Rev. B, 33 (1986) 7792-7794.

[9] N. Provatas, K. Elder, Phase-Field Methods in Materials Science and Engineering, Wiley-VCH, 2010.

[10] M. Greenwood, N. Provatas, J. Rottler, Phys. Rev. Lett., 105 (2010) 045702.

[11] M. Greenwood, N. Oforiopoku, J. Rottler, N. Provatas, Phys. Rev. B, 84 (2011) 1787-1794.

[12] X. Ren, J.C. Wang, Y.J. Yang, G.C. Yang, Acta. Phys. Sin-Ch Ed, 59 (2010) 3595-3600.

[13] K. Yang, Z. Chen, W.P. Dong, Y.X. Wang, M.Y. Zhang, Sci. China Technol. Sc., 54 (2011) 835-840.

[14] Q. Zhang, J.C. Wang, Y.C. Zhang, G.C. Yang, Acta. Phys. Sin., 60 (2011) 088104.

[15] T. Yang, Z. Chen, J. Zhang, W.P. Dong, L. Wu, Chinese Phys. Lett., 29 (2012) 078103.

[16] K.A. Wu, A. Adland, A. Karma, Phys. Rev. E., 81 (2010) 061601.

[17] J.W. Cahn, J.E. Hilliard, J. Chem. Phys., 28 (1958) 258-267.

[18] A. Jaatinen, C.V. Achim, K.R. Elder, T. Alanissila, Phys. Rev. E., 80 (2009) 031602.

[19] G. Tegze, L. Gránásy, G.I. Tóth, F. Podmaniczky, A. Jaatinen, T. Ala-Nissila, T. Pusztai, Phys. Rev. Lett., 103 (2009) 035702.

[20] P.F. Tupper, M. Grant, Epl, 81 (2008) 40007.